Comment on "Exploring potential energy surfaces to reach saddle points above convex regions" [J. Chem. Phys. 160, 232501 (2024)]

Wolfgang Quapp[1,*] and Josep Maria Bofill[2,3,†]

[1] *Mathematisches Institut, Universität Leipzig, PF 100920, D-04009 Leipzig, Germany*
[2] *Departament de Química Inorgànica i Orgànica, Secció de Química Orgànica*
[3] *Institut de Química Teòrica i Computacional (IQTCUB), Universitat de Barcelona, Martí i Franquès 1, 08028 Barcelona, Spain*

(Dated: October 22, 2024)

We comment on the work on convex regions of the potential energy surface (PES) of a molecule by M. Gunde; A. Jay; M. Poberžnik; N. Salles; N. Richard; G. Landa; N. Mousseau; L. Martin-Samos and A. Hemeryck [J. Chem. Phys. 160, 232501 (2024)]. In contrast to the activation-relaxation technique nouveau (ARTn), in the present work we apply the theory of Newton trajectories (NTs) to the 2D PES. NTs have no problem traversing convex or concave regions of the PES. The ARTn is compared with the Gentlest Ascent Dynamics method as well as with NTs.

I. INTRODUCTION

This letter concerns a mathematical detour which discusses the use of the activation-relaxation technique nouveau (ARTn) for a potential energy surface (PES), $V(\mathbf{x})$, with various convex regions [1]. In contrast, we use a curve $\mathbf{x}(t)$ where at each point the gradient of the PES is parallel to a given direction, $\mathbf{f}$

$$\mathbf{grad}(\mathbf{x}(t)) \quad || \quad \mathbf{f} \ , \tag{1}$$

t is a curve length parameter. Curves that solve Eq.(1) are of particular interest in mechanochemistry, where the direction $\mathbf{f}$ can be the direction of an external force [2–4]. It changes the PES in the simplest, linear case by the equation

$$V_{eff}(\mathbf{x}) = V(\mathbf{x}) - F\,\mathbf{f}\,\mathbf{x} \ . \tag{2}$$

where $\mathbf{f}$ is the normalized force direction, F is the force magnitude, and $\mathbf{f}$ and $\mathbf{x}$ form a scalar product. In Appendix I we demonstrate the effect of a mechanochemical force on a 2D PES.

The problem of Eq.(1) was formulated by Branin in a differential equation [5, 6]

$$\frac{d\mathbf{x}(t)}{dt} = Det(H(\mathbf{x}(t)))\ H^{-1}(\mathbf{x}(t))\,\mathbf{grad}(\mathbf{x}(t)) \ , \tag{3}$$

H is the Hessian of the second derivatives of the PES. It is important that the matrix

$$A \ = Det(H)\ H^{-1} \tag{4}$$

is desingularized when the Hessian becomes singular. The matrix A is called the adjoint matrix for H. The full Hessian matrix can be computationally expensive at each step of the positions $\mathbf{x}(t)$. However, it can be updated [7–11]. A first numerical step from a stationary point goes in direction $\mathbf{f}$. The following steps then secure that the gradient maintains this direction [6]. The solution curves are called Newton trajectories (NT).

NTs have the nice property that they connect stationary points with an index difference of one [6, 12], compare the example in Section II. If we start at a minimum, we obtain a next saddle point (SP) with index one. A special case is a singular NT that crosses a valley ridge inflection (VRI) point [6]. Normally it connects a minimum with a saddle of index two and two SPs of index one via the VRI. A VRI represents the branching of a valley. With these properties, we can fully investigate the toy PES in Ref.[1] as well as any high-dimensional PES. We can follow a one-dimensional curve by Eq. (3) in any dimension. Note that the number of steps to reach an SP depends mainly on the step length used, and of course on the length of the path from the minimum to this SP. So we do not need 'drastically different numbers of steps' [1] for different SPs.

The following of an NT is included in the COLUMBUS program system [13] (under the name reduced gradient following, RGF). There are some links to different programs [14–16]. The Newton trajectory method has been established in chemistry since 1998, see refs. [4, 17–23] and the references therein. We report that NTs are calculated for the PES of Frenkel-Kontorova chains with up to 500 atoms [24] and for medium molecules with up to 150 atoms [25]. Generalizations of the method for nonlinear forces are proposed instead of Eq. (2) [26].

In Section II we demonstrate the application of the theory of NTs for a 2D test PES. The conclusions are given in Section III. Appendix I demonstrates the application of a mechanochemical force, but Appendix II draws a comparison between ARTn, Gentlest Ascent Dynamics (GAD) and NTs.

A few notes in advance: To calculate the stationary points of the PES of a molecule, only $3N_{at}$-6 internal degrees of freedom (DoF) are needed.

A second gap is the wayward definition of a ridge on page 3 in Ref. [1]. For example, at an SP of index one

* quapp@math.uni-leipzig.de
† jmbofill@ub.edu

we have one negative eigenvalue of the Hessian but N-1 positive eigenvalues (if N is the dimension). If we go uphill from the SP perpendicular to the valley direction, we have positive curvature. This it is a (hyper)-ridge of dimension N-1. In Fig. 2 below, in the region around the maximum, the region with two negative eigenvalues is inside the green line around the maximum.

A third gap in the annotated paper is the lack of knowledge about the well known streambed methods such as gradient extremal following, see for example Refs.[27, 28].

A fourth gap in the commented work is the lack of knowledge about the Gentlest Ascent Dynamics (GAD) method, where the gradient of the PES is projected into a certain direction and also perpendicular to it, see for example Ref. [29]. ARTn is, so to speak, a special case of the GAD technique. Since this comment mainly describes that NTs can cross convex or concave regions of the PES equally, we provide an explanation of this point in Appendix II.

A further gap is the distinction between 'valley branching' and VRI points. This is not correct. Singular NTs unambiguously define the branching [6, 30–32]. There is an illustrative introduction to the higher dimensional case [33]. For a PES with more than two (toy) dimensions manifolds of VRI points arise [34]. If the PES is symmetric, the VRI manifold often forms a symmetry hypersurface. However, asymmetric VRI manifolds can also be computed [15, 34, 35]. Recently, the role of VRI points in dynamical processes has been discussed [36].

II. FIND THE SP OF AN EXAMPLE PES

The PES of Ref.[1] is

$$V(x,y) = \tfrac{1}{2}cos(\tfrac{xy}{5})\ cos(\tfrac{3x}{5})\ cos(\tfrac{y}{2}) + cos(x)\ cos(\tfrac{3y}{2}) + exp(-[(x-17)^2+(y-17)^2]/125) \quad (5)$$

for $x \in [13, 18]$ and $y \in [14.7, 18.6]$, as shown in Fig.1. There is a central minimum, M, which is surrounded by five SPs. Five VRI points are shown between the SPs through Xi, where i is a consecutive number. The boundaries of the convex-concave regions are enclosed by green lines. They are given by the condition $det(H) = 0$. These lines also cross the VRI points. Normally they are curvilinear, so that the points of a molecule on a higher dimensional PES with $det(H) = 0$ form curved hypersurfaces (not 'hyperplanes' as claimed in [1]).

Each VRI is intersected by its own singular NT, all of which are represented by thin blue lines. For example, the dashed blue curve is the singular NT through the VRI point X1. Singular NTs are the boundaries of families of NTs that connect the minimum, M, with different SPs. Two singular NTs each form a corridor for all NTs connecting the minimum, M, with the same SPi [37].

To find all SPs, you have to choose an appropriate direction in the corresponding corridor. For example, a branch of the thick black NT (direction $\mathbf{f}=\frac{1}{\sqrt{2}}(1,1)$) connects SP1 to M via Sh, which leads to SP4. A branch of the magenta NT ($\mathbf{f}$=(1,0)) connects SP3 with M and goes to SP5. Incidentally, it is not necessary to follow the specified NT exactly within a corridor, since a neighboring NT also leads to the same next stationary point.

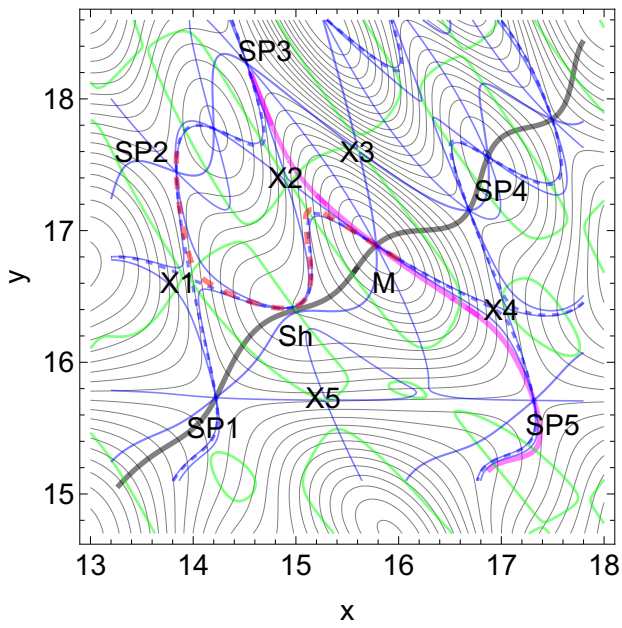

FIG. 1. Level lines (thin black) of the PES (5). M is the central minimum, SPi are the 5 closest transition states, but Xi are the 5 VRI points between the SPs. A special region is the shoulder, Sh. See the text for the meaning of each colored line.

The special region of this PES here is the shoulder, Sh, where some NTs come close to each other, but do not intersect [38]. The steepest descent from SP2 leads to the shoulder. To connect SP2 with the minimum, M, we have to find a direction between the blue singular NTs through VRI points $X1$ and $X2$. For example, this is fulfilled by the dashed red NT to direction $(0.987, 0.163)$. Before M, the red NT moves together with the magenta NT to SP5. This means that the corridors before M and after M are different.

Note that there is no bifurcation of the valley of M at the shoulder, Sh. The corresponding bifurcation points are $X1$ and $X5$, which are the boundary points for the corridor of the thick black NT from the minimum M to $SP1$.

The dashed red NT is also shown in an extended region of the PES in Fig. 2. The corridor for this NT is quite small. A boundary is the dashed blue singular NT through VRI point X1 on the left, but the other boundary is the blue singular NT through VRI point X2. It connects the minimum, Min, directly to X2 and the maximum, Max. Its other branch leads from X2 to the desired SP2, but in a large arc. The dashed red NT lies above and to the right of the dashed blue boundary, and below

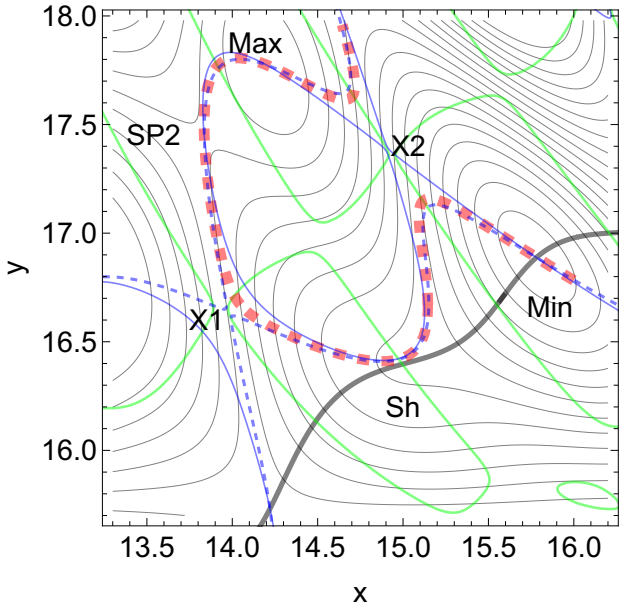

FIG. 2. Extended range of Fig. 1 to include the minimum, the shoulder, the VRI points X1 and X2, the SP2 and a maximum.

and to the left of the solid blue NT. Near the shoulder, Sh, all NTs come close to each other but do not cross, compare also Fig. 1 of ref. [39] where a similar situation is described.

One can observe in Fig. 2 the different convex or concave regions of the PES through which the dashed red NT passes, crossing the green lines. Around M the region is convex, near $X2$ up to Sh it is concave, between Sh and $X1$ it is convex again and then up to $SP2$ it is finally concave. This NT goes uphill through a valley from M to $SP2$.

Similarly, other singular NTs form other corridors to SPs numbered 1, 3, 4, or 5.

On this PES, the dashed red NT does not find the next minimum after SP2, but continues uphill to the maximum, an SP of index two, with two negative eigenvalues of the Hessian matrix. This is allowed by the property of regular NTs. They connect stationary points with an index difference of one [6, 12]. Here the NT moves from index one of SP2 to index two of the maximum. Note that saddles of index two have been discussed in chemistry since 1986 [40, 41]. Currently they play a role in the discussion about roaming atoms [42].

III. CONCLUSION

We propose to applied Newton trajectories that can immediately find all SPs of a given minimum basin, see Fig. (1a) of Ref. [1]. The special curvature of the PES does not matter [43]. The starting point does not need to be changed. All NTs to the five SPs around M start at M.

APPENDIX I

A mechanochemical example

We use the 2D PES Eq. (5) with the mechanochemical approach Eq.(2) with $\mathbf{f}$=(0.987, 0.163), the gradient direction of the dashed red NT in Figs. 1 and 2. For the original PES, SP1 and SP3 are lower than SP2, whith SP3 being the lowest. If we use an amount of $F = -0.25$ force units, we get the effective PES shown in Fig. 3.

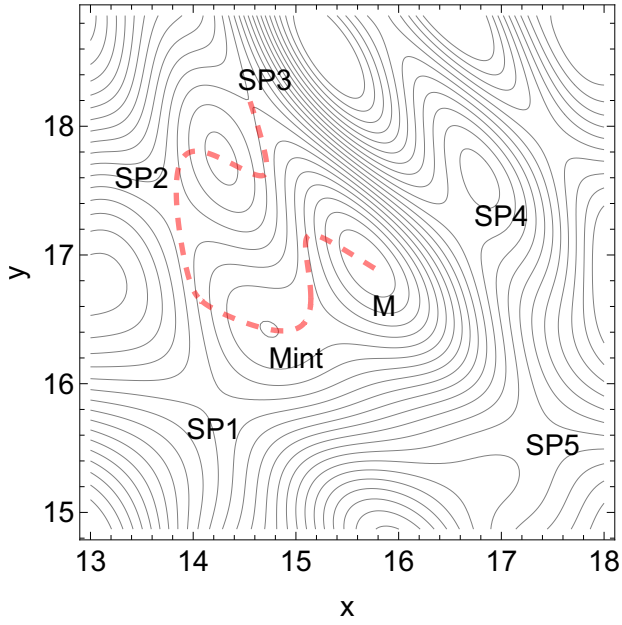

FIG. 3. Effective PES for a mechanochemical pull towards the dashed red NT with force $F = -0.25$. See text.

Now, SP1 and SP2 are lowered below SP3. If it is possible to pull a chemical system with this PES in the indicated direction, the high probability that a reaction will occur above SP3 can be changed to proceed above the SP1 and SP2. Note that the shoulder is now gone. A new intermediate minimum, $Mint$, is formed. One may also observe that the stationary points, M, Mint, SP2, Max, and SP3, are moving on the dashed, red NT. This is the key property for the application of NTs in mechanochemistry: NTs describe the motion of stationary points under the external force.

APPENDIX II

From the Scheraga method to the GAD model via ARTn and a comparative analysis with NTs

Scheraga proposed half a century ago the first algorithm for scaling and exploring a PES as well as to locate first-index saddle points [44]. The algorithm starts at an initial point $\mathbf{x}_0$ and in iteration k the system is at the point $\mathbf{x}_k$. The new point is found by minimizing the potential energy $V(\mathbf{x})$ on a hyperplane S_k whose normal

vector is $\mathbf{n}_k$. We always take the vector $\mathbf{n}_k$ normalized, $\mathbf{n}_k^T\mathbf{n}_k = 1$. The hyperplane is defined by

$$\mathbf{n}_k^T(\mathbf{x}_k^* - \mathbf{x}_k) = 0 \ , \tag{6}$$

where the points $\mathbf{x}_k^*, \mathbf{x}_k \in S_k$. Minimizing $V(\mathbf{x})$ on the hyperplane S_k perpendicular to $\mathbf{n}_k$ gives the new point by the formula

$$\mathbf{x}_{k+1} = \delta_k\mathbf{n}_k + \text{argmin}_{\mathbf{x}_k^*\in S_k}V(\mathbf{x}_k^*) \tag{7}$$

where $\delta_k > 0$. This is a parameter that must be adjusted at each iteration. The process is repeated until the system reaches the SP of index one. This algorithm is very general. It defines in a very basic way what any algorithm whose purpose is to find first-index saddle points on a PES must have. However, it suffers in two points: first, how to obtain $\mathbf{n}_k$ in each iteration and second, what it costs to minimize $V(\mathbf{x})$ in the hyperplane S_k.

Among many other algorithms proposed on the basis of Scheraga's, it is worth highlighting that of Barkena and Mousseau called the activation-relaxation method (ARTn) [45–48]. To see the connection between this algorithm and the more general Scheraga algorithm, we make the following modifications. We transform

$$\delta_k \to -\frac{\mathbf{n}_k^T\mathbf{g}(\mathbf{x}_k)}{\min(\lambda_k, -\beta_k)} \tag{8}$$

and

$$\text{argmin}_{\mathbf{x}_k^*\in S_k}V(\mathbf{x}_k^*) \to \mathbf{x}_k - \mu_k(\mathbf{I} - \mathbf{n}_k\mathbf{n}_k^T)\mathbf{g}(\mathbf{x}_k) \ . \tag{9}$$

The parameters, $\beta_k > 0$ and $\mu_k > 0$, are arbitrary and different for each iteration. λ_k is an eigenvalue of the Hessian. Instead of minimizing $V(\mathbf{x})$ in the hyperplane, this is replaced by a minimization of the gradient descent type in the subspace normal to the vector $\mathbf{n}_k$, i.e. in the subspace S_k. This computation is less expensive than minimizing $V(\mathbf{x})$. With these considerations, the general formula of Scheraga's algorithm for finding the new point $\mathbf{x}_{k+1}$ now has the following form

$$\mathbf{x}_{k+1} = \mathbf{x}_k - \frac{1}{\min(\lambda_k, -\beta_k)}\mathbf{n}_k(\mathbf{n}_k^T\mathbf{g}(\mathbf{x}_k)) \\ -\mu_k(\mathbf{I} - \mathbf{n}_k\mathbf{n}_k^T)\mathbf{g}(\mathbf{x}_k) \ . \tag{10}$$

The ARTn algorithm provides an unambiguous way to obtain the vector $\mathbf{n}_k$ from the the eigenvalue equation of the Hessian matrix, $\mathbf{H}(\mathbf{x}_k)\mathbf{n}_k = \lambda_k\mathbf{n}_k$, by taking the eigenvector of the smallest eigenvalue. These are the two equations that must be evaluated in each iteration of the ARTn algorithm. In Mousseau's last article the hyperplane was changed to a hypersphere, see Fig. 4 of ref. [1], but the methodological basis is the same.

At this point, it is worth highlighting that in the evolution of the algorithms based on the Scheraga model, the one with the most sophisticated of all is the one based on a dynamic formulation known as Gentlest Ascent Dynamics (GAD) [29, 49–54]. We can connect the GAD algorithm to the ARTn algorithm in the following way. We establish the relation

$$\frac{1}{\min(\lambda_k, -\beta_k)} \to -\Delta t_k \tag{11}$$

where $\Delta t_k = t_{k+1} - t_k > 0$ and we define $\Delta\mathbf{x}_k = \mathbf{x}_{k+1} - \mathbf{x}_k$. With these relations, the first ARTn equation has the following form

$$\Delta\mathbf{x}_k = -\Delta t_k(\mathbf{I} - 2\mathbf{n}_k\mathbf{n}_k^T)\mathbf{g}(\mathbf{x}_k) \ . \tag{12}$$

Regarding the second ARTn equation of the eigenvalues and eigenvectors of the Hessian matrix now has the form

$$\Delta\mathbf{n}_k = -\Delta t_k(\mathbf{I} - \mathbf{n}_k\mathbf{n}_k^T)\mathbf{H}(\mathbf{x}_k)\mathbf{n}_k \ , \tag{13}$$

where, $\Delta\mathbf{n}_k = \widetilde{\mathbf{n}}_{k+1} - \mathbf{n}_k$, and so

$$\mathbf{n}_{k+1} = \frac{\widetilde{\mathbf{n}}_{k+1}}{\|\widetilde{\mathbf{n}}_{k+1}\|} \ . \tag{14}$$

These two equations, which must be evaluated in each iteration, represent a very sophisticated and advanced form of Scheraga's original method. The GAD model is also an example of the optimally controlled Zermelo navigation problem [53, 54]. In this case, this is understood as navigation on the PES.

Finally, let us look at the analogies between the philosophy of Scheraga's method and the NT algorithm [12]. At the iteration k the Branin Eq. (3) [5] has the form

$$\Delta\mathbf{x}_k = \Delta t_k \, \|\mathbf{g}(\mathbf{x}_k)\| \left[\sum_{\nu=1}^{N} a_\nu^{(k)}\mathbf{v}_\nu^{(k)}\mathbf{v}_\nu^{(k)T}\right]\mathbf{n} \ , \tag{15}$$

with $\mathbf{g}(\mathbf{x}_k) = \mathbf{n}\,\|\mathbf{g}(\mathbf{x}_k)\|$, and where $\{a_\nu^{(k)}\}_{\nu=1}^N$ are the eigenvalues of the adjoint Hessian of Eq. (4) in the iteration k and $\{\mathbf{v}_\nu^{(k)}\}_{\nu=1}^N$ are its eigenvectors. Therefore, the computation of this equation involves the computation of the Hessian matrix and its eigenvalue and eigenvector equations, hence

$$\mathbf{H}(\mathbf{x}_k)\mathbf{v}_\nu^{(k)} = \lambda_\nu^{(k)}\mathbf{v}_\nu^{(k)} \tag{16}$$

in the same way as it occurs in the ARTn algorithm. We use the normalized eigenvectors, $\mathbf{v}_\nu^{(k)T}\mathbf{v}_\nu^{(k)} = 1$. With all this, we can calculate the elements

$$a_\nu^{(k)} = \frac{det(\mathbf{H}(\mathbf{x}_k))}{\lambda_\nu^{(k)}} \ . \tag{17}$$

This represents an NT iteration. To see the analogy with the previous algorithms we consider that
if $\lambda_1^{(k)} < 0$ and $\lambda_\nu^{(k)} > 0$, $\quad \nu = 2, \ldots, N$,
then it is $a_1^{(k)} > 0$ and $a_\nu^{(k)} < 0$, $\quad \nu = 2, \ldots, N$.
(This excludes the zero eigenvalues of the overall DoF.

In convex regions of the PES, they should be the lowest ones.)

With the previous considerations, the Branin Eq. (3) can be rewritten as follows

$$\Delta \mathbf{x}_k = \Delta t_k \, \|\mathbf{g}(\mathbf{x}_k)\| \left(a_1^{(k)} \mathbf{v}_1^{(k)} \mathbf{v}_1^{(k)T} - \sum_{\nu=2}^{N} |a_\nu^{(k)}| \mathbf{v}_\nu^{(k)} \mathbf{v}_\nu^{(k)T} \right) \mathbf{n} \quad (18)$$

which is very similar to the first equation of the ARTn algorithm, but it is more flexible by explicitly using the projectors, $\mathbf{v}_\nu^{(k)} \mathbf{v}_\nu^{(k)T}$, instead of using only two projectors and the contribution of elements $a_\nu^{(k)}$. This allows the NT algorithm to locate VRI points [34] which is not possible for an ARTn type algorithm.

We emphasize that all previously discussed and analyzed methods using the Hessian matrix can be updated and diagonalized by the method described in Ref. [8]. This work is an oriented and focused method for large molecular systems.

Conflict of Interest: We declare that we have no affiliation with or involvement in any organization that has financial interest in the subject matter or materials discussed herein.

Author Contributions: WQ and JMB contributed equally.

Methods: We have used Mathematica 13.3.1.0 for Linux x86(64-bit) in the calculations and in the representation of the figure.

Data Access Statement: All relevant data are included in the paper. Further data can be obtained from WQ.

Acknowledgements: Spanish Structures of Excellence María de Maeztu Program, Grant CEX2021-001202-M, Agència de Gestió d'Ajuts Universitaris

[1] M. Gunde, A. Jay, M. Poberžnik, N. Salles, N. Richard, G. Landa, N. Mousseau, L. Martin-Samos, and A. Hemeryck, *Exploring potential energy surfaces to reach saddle points above convex regions*, J. Chem. Phys. **160**, 232501 (2024).

[2] W. Quapp and J. M. Bofill, *A contribution to a theory of mechanochemical pathways by means of newton trajectories*, Theoret. Chem. Acc. **135**, 113 (2016).

[3] W. Quapp and J. M. Bofill, *Towards a theory of mechanochemistry- simple models from the very beginning*, Int. J. Quant. Chem. **118**, quae5775 (2018).

[4] W. Quapp and J. M. Bofill, *Theory and examples of catch bonds*, J. Phys. Chem. B **128**, 4097–4110 (2024).

[5] F. H. Branin, *Widely convergent methods for finding multiple solutions of simultaneous nonlinear equations*, IBM J. Res. Develop. **16**, 504–522 (1972).

[6] W. Quapp, M. Hirsch, and D. Heidrich, *Bifurcation of reaction pathways: the set of valley ridge inflection points of a simple three-dimensional potential energy surface*, Theor. Chem. Acc. **100**, 285–299 (1998).

[7] J. M. Bofill, *Updated Hessian matrix and the restricted step method for locating transition structures*, J. Comput. Chem. **15**, 1–11 (1994).

[8] J. M. Anglada, E. Besalú, J. M. Bofill, and J. Rubio, *Another way to implement the Powell formula for updating Hessian matrices related to transition structures*, J. Math. Chem. **25**, 85–92 (1999).

[9] H. P. Hratchian and H. B. Schlegel, *Using Hessian updating to increase the efficiency of a Hessiian based predictor-corrector relation path following method*, Journ. Chem. Theory Comput. **1**, 61 (2005).

[10] H. P. Hratchian and H. B. Schlegel, in *Theory and Applications of Computational Chemistry*, edited by C. E. Dykstra, G. Frenking, K. S. Kim, and G. E. Scuseria (Elsevier, Amsterdam, 2005) pp. 195–249.

[11] O. M. Lecian, *Generalisations of the Bofill update*, Int. J. Math. Computer Res. **11**, 3734–3739 (2023).

[12] J. M. Bofill and W. Quapp, *Variational nature, integration, and properties of the Newton reaction path*, J. Chem. Phys. **134**, 074101 (2011).

[13] COLUMBUS, *program system*, https://columbus-program-system.gitlab.io/columbus/ (2023).

[14] W. Quapp, *Program: growing string method for Newton trajectories*, https://www.math.uni-leipzig.de/∼quapp/gs2teord/gs2teord.html (2009).

[15] W. Quapp, *Program for unsymmetric valley-ridge inflection points*, https://www.math.uni-leipzig.de/∼quapp/SkewVRIs.html (2011).

[16] W. Quapp, *Mathematica notebook for catch bond calculations*, https://community.wolfram.com/groups/-/m/t/3167380 , **Wolfram** (2024).

[17] J. Gonzalez, X. Gimenez, and J. M. Bofill, *A reaction path Hamiltonian defined on a Newton path*, J. Chem. Phys. **116**, 8713–8722 (2002).

[18] R. Crehuet and J. M. Bofill, *The reaction path intrinsic reaction coordinate method and the Hamilton-Jacobi theory*, J. Chem. Phys. **122**, 234105–234120 (2005).

[19] W. Quapp, *A growing string method for the reaction pathway defined by a Newton trajectory*, J. Chem. Phys. **122**, 174106 (2005).

[20] S. S. M. Konda, J. M. Brantley, C. W. Bielawski, and D. E. Makarov, *Chemical reactions modulated by mechanical stress: Extended Bell theory*, J. Chem. Phys. **135**, 164103 (2011).

[21] D. Mehta, T. Chen, J. W. R. Morgan, and D. J. Wales, *Exploring the potential energy landscape of the Thomson problem via Newton homotopies*, J. Chem. Phys. **142**, 194113 (2015).

[22] T. M. Cardozo, A. P. Galliez, I. Borges Jr, F. Plasser, A. J. A. Aquino, M. Barbatti, and H. Lischka, *Dynamics of benzene excimer formation from the parallel-displaced dimer*, Phys. Chem. Chem. Phys. **21**, 13916–13924 (2019).

[23] C. O. Barkan and R. F. Bruinsma, *Topology of molecular deformations induces triphasic catch bonding in selectin-ligand bonds*, Proc. Natl. Acad. Sci. **121**, e2315866121 (2024).

[24] W. Quapp and J. M. Bofill, *An analysis of some proper-*

ties and of the use of the twist map for the finite Frenkel-Kontorova model, Electronics **11**, 3295 (2022).

[25] W. Quapp, *Finding the transition state without initial guess: the growing string method for Newton trajectory to isomerisation and enantiomerisation reaction of alanine dipeptide and poly(15)alanine*, J. Comput. Chem **28**, 1834–1847 (2007).

[26] J. M. Bofill, W. Quapp, G. Albareda, I. de P. R. Moreira, and J. Ribas-Ariño, *A model for an optimally oriented external electric field to control the chemical reaction path: A generalisation of the Newton trajectory*, J. Chem. Theor. Comput. **18**, 935–952 (2022).

[27] D. K. Hoffmann, R. S. Nord, and K. Ruedenberg, *Gradient extremals*, Theor. Chim. Acta **69**, 265–280 (1986).

[28] J. M. Bofill, W. Quapp, and M. Caballero, *The variational structure of gradient extremals*, J. Chem. Theory Comput. **8**, 927–935 (2012).

[29] J. M. Bofill, J. Ribas-Arino, R. Valero, G. Albaredo, I. d. Moreire, and W. Quapp, *Interplay between the gentlest ascent dynamics method and conjugate directions to locate transition states*, J. Chem. Theo. Comput. **15**, 5426–5439 (2019).

[30] T. Taketsugu, T. Yanai, K. Hirao, and M. S. Gordon, *Dynamic reaction path study of SiH4+F- → SiH4F- and the Berry pseudorotation with valley-ridge inflection*, J. Molec. Struc.: THEOCHEM **451**, 163–177 (1998).

[31] W. Quapp and V. Melnikov, *The set of valley ridge inflection points on the potential energy surfaces of h2s, h2se and h2co*, Phys. Chem. Chem. Phys. **3**, 2735–2741 (2001).

[32] W. Quapp, M. Hirsch, and D. Heidrich, *An approch to reaction path branching using valley-ridge-inflection points of potential energy surfaces*, Theor. Chem. Acc. **112**, 40–51 (2004).

[33] W. Quapp, *Can we understand the branching of reaction valleys for more than two degrees of freedom?*, J. Math. Chem. **54**, 137–148 (2015).

[34] J. Bofill and W. Quapp, *Analysis of the valley-ridge inflection points through the partitioning technique of the Hessian eigenvalue equation*, J. Math. Chem. **51**, 1099–1115 (2013).

[35] W. Quapp and B. Schmidt, *An empirical, variational method of approach to unsymmetric valley-ridge inflection points*, Theor. Chem. Acc. **128**, 47–61 (2011).

[36] V. J. García-Garrido and S. Wiggins, *The dynamical significance of valley-ridge inflection points*, Chem. Phys. Lett. **781**, 138970 (2021).

[37] M. Hirsch and W. Quapp, *Reaction Channels of the Potential Energy Surface: Application of Newton Trajectories*, J. Molec. Struct., THEOCHEM **683**, 1–13 (2004).

[38] M. Hirsch and W. Quapp, *The reaction pathway of a Potential Energy surface as curve with induced tangent*, Chem. Phys. Lett. **395**, 150–156 (2004).

[39] W. Quapp and J. M. Bofill, *A model for a driven Frenkel-Kontorova chain*, Eur. Phys. J. B **92**, 95–117 (2019).

[40] D. Heidrich and W. Quapp, *Saddle points of index 2 on PES and their role in theoretical reactivity investigations*, Theor. Chem. Acc. **70**, 89–98 (1986).

[41] R. M. Minyaev, I. V. Getmanskii, and W. Quapp, *Ab initio study of the NH_3...H_2 complex- first saddle point of index two on a reaction path*, Russ. J. Phys. Chem. **78**, 1494 (2004).

[42] H. Cao and S. Wiggins, *Phase space reaction dynamics associated with an index-2 saddle point for time-dependent Hamiltonian systems*, Int. J. Bifurcat. Chaos **32**, 2230036 (2022).

[43] M. Hirsch and W. Quapp, *Reaction pathways and convexity of the potential energy surface: Application of Newton trajectories*, J. Math. Chem. **36**, 307–340 (2004).

[44] G. M. Crippen and H. A. Scheraga, *Minimization of polypeptide energy. XI. the method of gentlest ascent*, Arch. Biochem. Biophys. **144**, 462–466 (1971).

[45] G. T. Barkena and N. Mousseau, *Event-based relaxation of continuous disordered systems*, Phys. Rev. Lett. **77**, 4358 (1996).

[46] N. Mousseau and G. T. Barkema, *Activated mechanisms in amorphous silicon: An activation-relaxation-technique study*, Phys. Rev. B **61**, 1898 (2000).

[47] E. Cancès, F. Legoll, M.-C. Marinica, K. Minoukadeh, and F. Willaime, *Some improvements of the activation-relaxation technique method for finding transition pathways on potential energy surfaces*, J. Chem. Phys. **130**, 114711 (2009).

[48] M.-C. Marinica, F. Willaime, and N. Mousseau, *Energy landscape of small clusters of self-interstitial dumbbells in iron*, Phys. Rev. B **83**, 094119 (2011).

[49] W. E and X. Zhou, *The gentlest ascent dynamics*, Nonlinearity **24**, 1831–1842 (2011).

[50] A. Samanta and W. E, *Atomistic simulations of rare events using gentlest ascent dynamics*, J. Chem. Phys. **136**, 124104 (2012).

[51] J. M. Bofill, W. Quapp, and M. Caballero, *Locating Transition States on Potential Energy Surfaces by the Gentlest Ascent Dynamics*, Chem. Phys. Lett. **583**, 203–208 (2013).

[52] W. Quapp and J.M.Bofill, *Locating saddle points of any index on potential energy surfaces by the generalized gentlest ascent dynamics*, Theor. Chem. Acc. **133**, 1510 (2014).

[53] J. M. Bofill and W. Quapp, *The variational nature of the gentlest ascent dynamics and the relation of a variational minimum of a curve and the minimum energy path*, Theor. Chem. Acc. **135**, 11–24 (2016).

[54] G. Albareda, J. M. Bofill, I. d. Moreira, W. Quapp, and J. Rubio-Martinez, *Exploring potential energy surfaces with gentlest ascent dynamics in combination with the shrinking dimer method and newtonian dynamics*, Theoret. Chem. Acc. **137**, 73–82 (2018).